

Journal of Materials Chemistry A

Accepted Manuscript



This is an *Accepted Manuscript*, which has been through the Royal Society of Chemistry peer review process and has been accepted for publication.

Accepted Manuscripts are published online shortly after acceptance, before technical editing, formatting and proof reading. Using this free service, authors can make their results available to the community, in citable form, before we publish the edited article. We will replace this *Accepted Manuscript* with the edited and formatted *Advance Article* as soon as it is available.

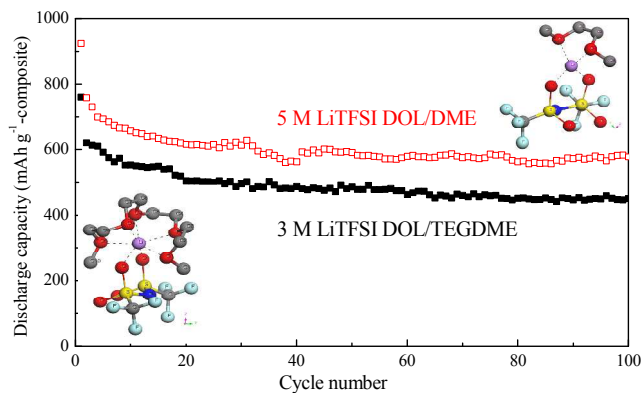
You can find more information about *Accepted Manuscripts* in the [Information for Authors](#).

Please note that technical editing may introduce minor changes to the text and/or graphics, which may alter content. The journal's standard [Terms & Conditions](#) and the [Ethical guidelines](#) still apply. In no event shall the Royal Society of Chemistry be held responsible for any errors or omissions in this *Accepted Manuscript* or any consequences arising from the use of any information it contains.

Sulfur/polyacrylonitrile/carbon multi-composites as cathode materials for lithium/sulfur battery in the concentrated electrolyte

Y. Z. Zhang, S. Liu, G. C. Li, G. R. Li, and X. P. Gao

TOC



The sulfur/polyacrylonitrile(PAN)/carbon multi-composite as active materials present the good electrochemical performance in the optimized electrolyte by the common ion effect and viscosity, which are induced from both the lithium salt and solvent.

Cite this: DOI: 10.1039/c0xx00000x

www.rsc.org/xxxxxx

Sulfur/polyacrylonitrile/carbon multi-composites as cathode materials for lithium/sulfur battery in the concentrated electrolyte

Y. Z. Zhang, S. Liu, G. C. Li, G. R. Li, and X. P. Gao*

Received (in XXX, XXX) Xth XXXXXXXXXX 20XX, Accepted Xth XXXXXXXXXX 20XX

DOI: 10.1039/b000000x

Sulfur/polyacrylonitrile(PAN)/carbon multi-composites with different sulfur content are prepared based on dual-mode of fixing sulfur on the matrix of the partially carbonized PAN (cPAN) and activated-conductive carbon black (A-CCB). The electrochemical performance of the as-prepared multi-composites as active materials are tested in the electrolyte with a high concentration lithium salt (LiTFSI) in different mixed solvents of 1,3-dioxolane (DOL)/1,2-dimethoxyethane (DME), and 1,3-dioxolane (DOL) /tetraethylene glycol dimethyl ether (TEGDME), respectively. It is demonstrated that the high concentration lithium salt (LiTFSI) and high viscous solvent have a great impact on the cycle stability of the multi-composite by suppressing polysulfide dissolution at the slight expense of the discharge potential plateaus (width and height). The as-prepared multi-composites present the excellent cycle performance in the electrolyte with 5 M LiTFSI in DOL/DME. Meanwhile, when the lower viscous DME solvent is replaced by the higher viscous TEGDME solvent in the electrolyte with 3 M LiTFSI, the optimized cycle stability is still obtained for the as-prepared multi-composites based on the evaluation of the discharge capacity and cycle stability. Therefore, the electrochemical performance of the as-prepared multi-composites is obviously influenced by the common ion effect and viscosity of the electrolyte, which are induced from both the lithium salt and solvent.

Introduction

Rechargeable lithium/sulfur (Li/S) battery is regarded as one of the most attractive candidates for high energy power sources as element sulfur is a low-cost, abundant cathode material with the large theoretical capacity of 1675 mAh g⁻¹, and Li/S battery possesses the larger theoretical energy density of 2600 Wh kg⁻¹.¹⁻⁵ Although, the significant progress has been made for the research of the Li/S battery in recent years, especially for the sulfur cathode. However, the practical development of key cathode materials for the Li/S battery is still limited because of some well-known drawbacks, including the highly insulating nature of sulfur (5×10⁻³⁰ S cm⁻¹ at 25 °C) and the high solubility of lithium polysulfides, leading to the poor coulombic efficiency, low utilization and poor cycle stability of the sulfur active material.⁶⁻⁷

In order to improve the electrochemical performance of sulfur cathode, elemental sulfur is usually loaded into the mesoporous/microporous carbon,⁸⁻¹⁹ or coated with conductive polymer,²⁰⁻²⁵ or fabricated with carbon and conductive polymer to form multi-composites,²⁶⁻³² based on the physical and chemical interaction for fixing sulfur on the matrix. In particular, it is demonstrated that sulfur can be strongly fixed on the p-conjugated co-plane hetero-ring of polyacrylonitrile (PAN)-derived backbone by heating a mixture of PAN and sulfur, resulting in good cycle stability of sulfur-based composites.^{20,33-35}

To further increase the sulfur content and discharge potential plateaus of sulfur-based composites, S/PAN can be incorporated with graphene^{28, 36} and metal oxide³⁷ to form multi-composites. In deed, as cathode for Li/S battery, such multi-composites do present the improved electrochemical performance. Meanwhile, it is shown from recent investigations that the suitable electrolyte is very important for the utilization and the cycle stability of the sulfur active material. Especially, the dissolution of lithium polysulfides from the sulfur cathode can be controlled based on the common ion effect and high viscosity in electrolyte with concentrated Li salts³⁸⁻⁴¹ and suitable solvents.⁴²⁻⁴⁴

It is noted from the previous results that carbon materials are shown to be more effective for improving the cycle stability, active sulfur utilization and high-rate capability of the sulfur cathode, due to their good electrical conductivity, and porous structure for loading active sulfur. In addition, the high sulfur loading is also indispensable for increasing the capacity of sulfur cathode and energy density of lithium/sulfur battery. To meet the requirements for practical application, in this work, we present dual-mode for fixing sulfur on partially carbonized PAN (cPAN) and activated-conductive carbon black (A-CCB) to fabricate S/cPAN/A-CCB multi-composites with different sulfur content. The electrochemical performance of the S/cPAN/A-CCB multi-composites is investigated in the concentrated electrolyte with different concentration lithium salt and solvent.

Experimental

Preparation and characterization

The commercial conductive carbon black (Black Pearls 2000, Cabot Corporation) was activated with KOH, denoted as A-CCB. The partially carbonized PAN (cPAN) was prepared by heating PAN (Mw=150000) to 250 °C with a heating rate of 5 °C min⁻¹ in a tube furnace and keeping at 250 °C for 0.5 h under air, and then cooled to room temperature. The mixture of the as-prepared cPAN and sublimed sulfur with the weight ratio of 4:6 was ball-milled in a planetary-type ball mill at a rotate-speed of 300 rpm for 5 h in ethanol medium. After drying at 50 °C for 6 h, to prepare S/cPAN, the mixture was heated to 350 °C at a heating rate of 5 °C min⁻¹ and kept at 350 °C for 5 h in a sealed stainless steel vessel filled with Ar. Then, S/cPAN (0.14g), A-CCB (0.06) and sodium sulfide solution (Na₂S₄, 40 wt %) were dissolved in a water-ethanol mixture (water/ethanol, v/v=9/1) with hexadecyl trimethyl ammonium bromide (CTAB, 0.05M) and ultrasonically treated for 1 h. Subsequently, the formic acid solution (HCOOH, 0.5 mol L⁻¹) was titrated drop-wise into the above solution with constant stirring for 3 h at room temperature. The resulting suspension was filtered and washed repeatedly with alcohol and de-ionized water until the solution became transparent. The mixture was dried in a vacuum oven at 60 °C for 12 h and heated at 155 °C for 12 h in a sealed stainless steel vessel filled with Ar. The temperature was then further increased to 300 °C and kept at 300 °C for 1 h. Finally, the S/cPAN/A-CCB multi-composites with different sulfur content were obtained after cooling down to room temperature. The sulfur content in the multi-composites was detected using a thermogravimetric analyzer (Mettler Toledo, TGA/DSC1) under Ar atmosphere with a flow rate of 50 mL min⁻¹ at a heating rate of 10 °C min⁻¹ from 30 to 800 °C. The microstructure and morphology of the samples were measured by Fourier transform infrared (FTIR) spectra (Tensor 27, Bruker), X-ray diffraction (XRD, Rigaku MiniFlex II) and transmission electron microscopy (TEM, FEI Tecnai F20).

Electrochemical measurement

In order to prepare the working electrode, the multi-composite was mixed with acetylene black and polytetrafluorethylene (PTFE) in a weight ratio of 70:20:10 with ethanol as dispersant. Subsequently, the paste was compressed into a thin piece with a roller. The as-obtained piece was cut into a disk film of 8 mm in diameter, which was dried in a vacuum oven at 50 °C for 12 h. The half-cells were assembled in an argon-filled glove box. Lithium metal foil was used as the counter electrode as well as the reference electrode, and the microporous polypropylene film (Celgard 2300) was used as a separator. The electrolytes were prepared in a glove box filled with highly purified argon by dissolving 0.2 M anhydrous lithium nitrate (analytical grade) and 1 M, 3 M, 5 M bis(trifluoromethanesulfonyl) imide (LiTFSI) in mixed solvents of 1,3-dioxolane (DOL)/1,2-dimethoxyethane (DME), and 1,3-dioxolane (DOL)/tetraethylene glycol dimethyl ether (TEGDME) by volume ratio of 1:1, respectively. All of the electrolyte lithium salts, solvent and additive were purchased from the J&K Scientific Ltd. (Beijing) and used without further treatment. Charge and discharge tests were performed galvanostatically to evaluate the electrochemical capacity and cycle stability based on the multi-composites as the active

materials between 3.0 and 1.5 V (versus Li/Li⁺) at ambient temperature using a LAND-CT2001A instrument (Wuhan Jinnuo, China). The cyclic voltammetry (CV) measurements were conducted with the CHI 600A electrochemical workstation (Shanghai ChenHua, China) at a scan rate of 0.1 mV s⁻¹. The shear viscosity of the electrolyte was measured using an Anton Paar Physica MCR 301 rheometer with the shear rate of 100 s⁻¹ at 25 °C. Ionic conductivity measurements were performed at 25 °C, using a conductivity apparatus (DDS-12B, Tianjin) and platinum black electrodes.

Results and discussion

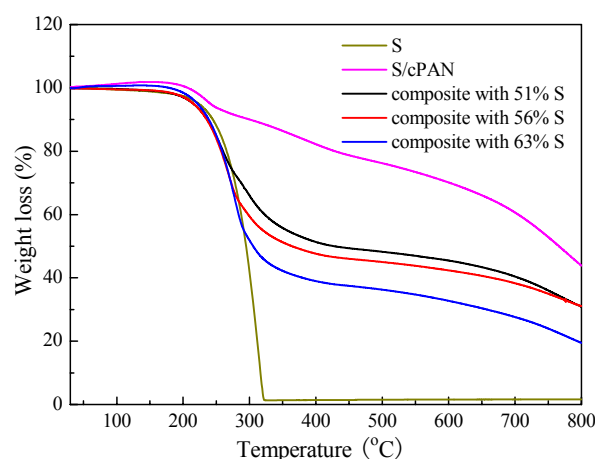


Fig. 1 TG curves of the as-prepared S/cPAN/carbon multi-composites, S/cPAN and sulfur, recorded under Ar atmosphere.

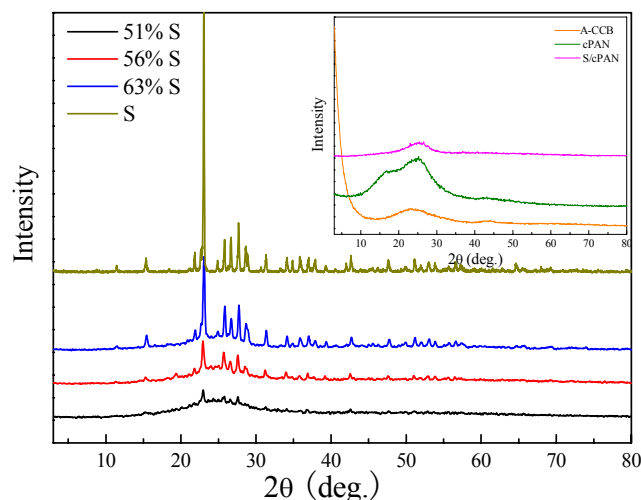


Fig. 2 XRD patterns of the as-prepared S/cPAN/carbon multi-composites, cPAN, S/cPAN and sulfur.

The sulfur content of the composites is measured by thermogravimetric analysis (TG) under flowing Ar atmosphere with a heating rate of 10 °C min⁻¹ from 30 to 800 °C, as shown in Fig. 1. The weight of the pure sulfur is rapidly decreased as the temperature increases from 180 °C and finished at about 320 °C. In the case of the as-prepared multi-composites, the weight loss is rather slow, and there is two-step process for the sulfur evaporation. Firstly, the weight loss of the sulfur is obviously

sharp with increasing temperature from about 180 °C, and the curves become stable when the composites are heated over 400 °C due to evaporation of sulfur from the mesopores or micropores of the host A-CCB. With further increasing temperature from 400 °C, the weight loss is rather slow, which is attributed to the interaction between sulfur and PAN with a relatively stable structure.³³ The sulfur content of the as-prepared multi-composites are 51, 56 and 63 wt %, respectively, calculated roughly from the TG curves, since vulcanized PAN may lose nitrogen and hydrogen together with sulfur in the temperature range of 320 to 800 °C. Correspondingly, in order to avoid measurement error of the discharge capacity, the composite is used as the active material, instead of sulfur.

XRD patterns of the as-prepared S/cPAN/carbon multi-composites, cPAN, S/cPAN and sulfur are presented in Fig. 2. Two broad diffraction peaks located at around 25 and 43° are shown for A-CCB, suggesting that A-CCB has a turbostratic structure with a large curvature of the graphite layer.⁴⁵ After heating at 250 °C, PAN is partially carbonized (cPAN) as demonstrated in the XRD pattern with two broad diffraction peaks of around 17 and 25.9°, corresponding to diffractions of (010) plane of PAN^{33,36} and parallel-oriented fragments of carbon layers, respectively. Also, it means that the carbonization of PAN at 250 °C is an incomplete cyclization process.³⁵ When sulfur is individually combined with cPAN, only a broad peak can be observed at 25° without appearance of characteristic peaks of both the crystalline sulfur and cPAN, indicating that sulfur becomes amorphous and homogeneously distributed in the cPAN matrix.³⁶ For the as-prepared multi-composites, clearly, weak characteristic peaks of the crystalline sulfur can be identified with a low intensity. It is believed that the most of sulfur diffuses into the pores of the host A-CCB and cPAN matrix, existing in highly dispersed or amorphous state.⁴⁵ However, the extra sulfur enclosed on the matrix may exist in nano-crystalline state due to re-crystallization in the as-prepared multi-composites. More detailed structure is presented in TEM images.

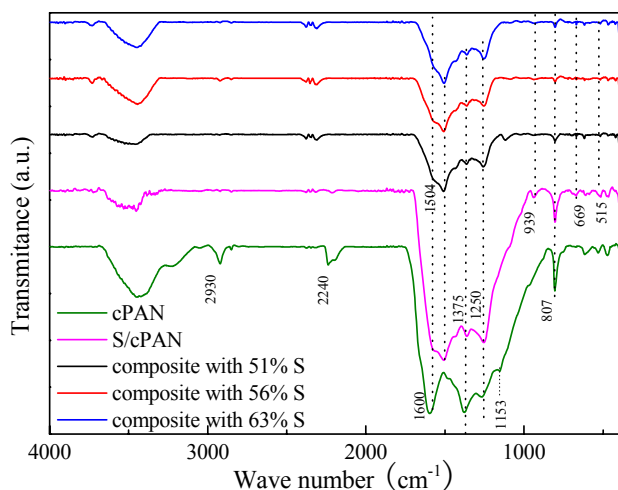


Fig. 3 FTIR spectra of the as-prepared S/cPAN/carbon multi-composites, cPAN, and S/cPAN.

FTIR spectra are presented here to demonstrate the interaction of the sulfur and matrix in the as-prepared multi-composites, as

shown in Fig. 3. Typically, the absorption peaks in cPAN may be attributed to the following bonds: CH₂ (2930 cm⁻¹), stretching vibrations of C≡N (2240 cm⁻¹), the stretching vibrations of double bonds (C=C, C=N and C-C=C-N (1600 cm⁻¹)), the vibration of C=N or C-H (1375 cm⁻¹), C-H (1250 cm⁻¹), and =CH (807 cm⁻¹), respectively. The absorption peaks of CH₂, C≡N, the stretching vibrations of double bonds (C=C, C=N and C-C=C-N), the vibration of C=N or C-H, C-H, and =CH are still found in the spectrum of S/cPAN, although the intensity of such peaks is reduced obviously. Additionally, some functional groups of C=C (1504 cm⁻¹) of the aromatic ring, S-S (515 and 939 cm⁻¹) and C-S (669 cm⁻¹)^{24,46} are also detectable after thermally treating cPAN and sulfur at 350 °C, implying that that sulfur can be chemically bonded with the PAN-derived backbone.²⁴ In the case of the as-prepared multi-composites, no distinct changes can be observed, indicating that no extra chemical reactions take place in the multi-composites.

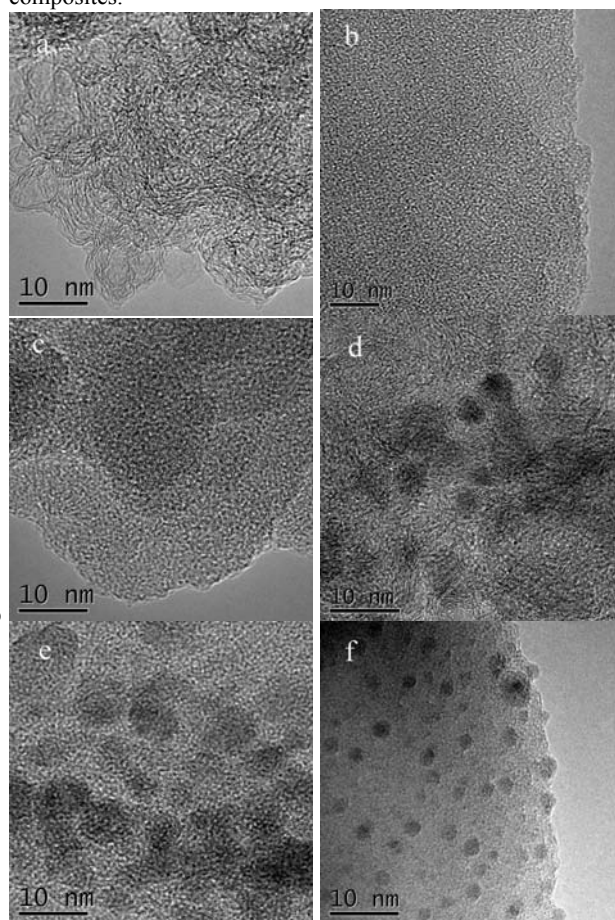


Fig. 4 TEM images of A-CCB (a), cPAN(b), S/cPAN(c) and the multi-composites with 51 wt % S (d), 56 wt % S (e) and 63 wt % S (f).

Fig. 4 shows TEM images of the multi-composites as well as the A-CCB, cPAN, and S/cPAN. The partially graphitized structure with some micropores/mesopores is observed in chain-like and interlaced nano-particles of the A-CCB,⁴⁵ which can ensure good conductivity of the carbon matrix. In the TEM image of cPAN (Fig. 4b), a narrow micropore size distribution of less than 0.7 nm is shown with a partially graphitized structure, coincident with the XRD analysis. After incorporating sulfur with cPAN, the uniform micropores on the matrix are still dominant

(Fig. 4c), almost the same as that of the cPAN matrix. Meanwhile, there is no crystalline sulfur can be observed from TEM image due to the highly uniform distribution of sulfur inside pores, as well as the low mass contrast between carbon and sulfur. When the sulfur is further loaded into S/cPAN and A-CCB to form multi-composites, some small crystalline sulfur nanoparticles (dark dots) appear clearly based on the mass-thickness contrast, due to the crystallization of extra sulfur inside pores or on the surface of the matrix of both cPAN and A-CCB (Fig.4d-f). In particular, the number of sulfur nanoparticles is apparently increased with increasing the sulfur content in the multi-composites. It means that the extra sulfur is compelled to aggregate and crystallize as nanoparticles on the surface of the matrix after preferably filling sulfur as the highly dispersed state into the pores of both cPAN and A-CCB, consistent with XRD analysis as shown in Fig.2. Therefore, the dual-mode of fixing sulfur is conducted in the multi-composites with chemically bonding to the PAN-derived backbone and physically loading on the matrix of both cPAN and A-CCB.

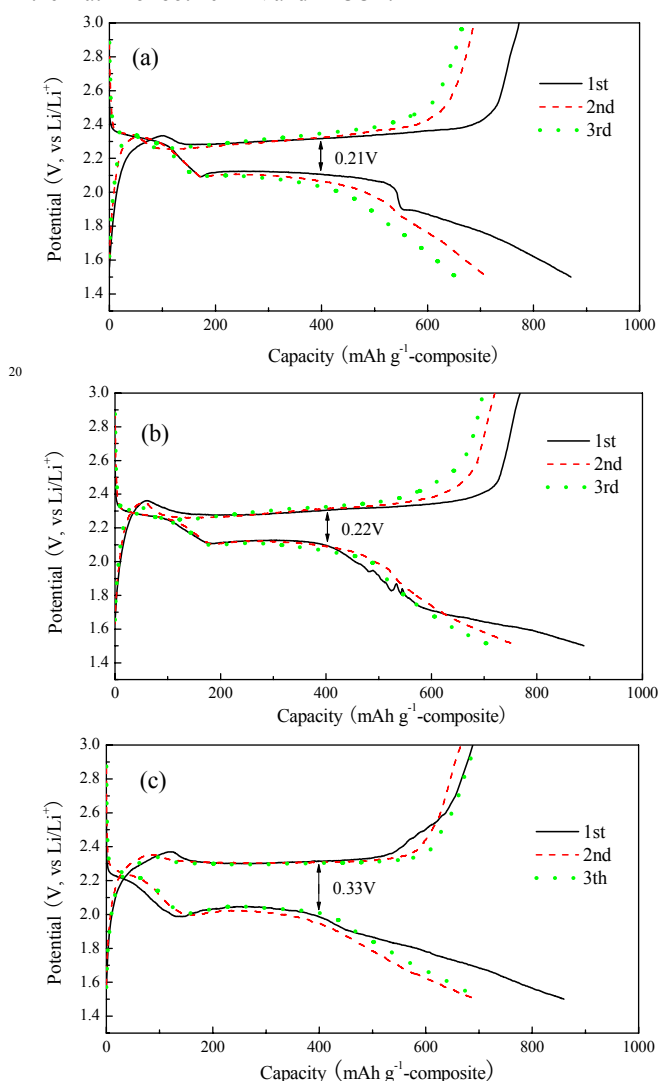


Fig. 5 The initial three charge–discharge curves of the as-prepared multi-composite with 51 wt % S at the current density of 100 mA g^{-1} in the electrolyte with 1 M LiTFSI (a), 3 M LiTFSI (b), and 5 M LiTFSI (c) in DOL/DME.

The initial three charge and discharge curves of the as-prepared multi-composite with 51 wt % S are shown in Fig. 5, measured in the electrolyte with different concentrated lithium salts (LiTFSI) in DOL/DME. There are two typical discharge potential plateaus at about 2.12 and 2.33 V (vs Li/Li⁺) with a hysteretic slope in the initial cycle for the multi-composite with 51 wt % S in the electrolyte with 1 M LiTFSI, which can be assigned to the reduction from sulfur to high-order lithium polysulfides as well as the further reduction to low-order lithium polysulfides and even to lithium sulfides in the end.^{7,9} The presence of the hysteretic slope in the discharge processes is mainly attributed to the existence of the chemical interaction between carbon and sulfur in the S-cPAN as shown in FTIR spectra. Only one potential plateau is presented in the charge process at about 2.30 V (vs Li/Li⁺), which is attributed to the interlaced conversion from lithium sulfides to low-order lithium polysulfides, high-order lithium polysulfides and sulfur. When the lithium salt concentration is increased to 3 and 5 M (LiTFSI), two discharge potential plateaus with a hysteretic slope can still be observed. However, the upper discharge potential plateau is reduced and is decreased from 2.33 V to 2.27 and 2.21 V (vs Li/Li⁺), while the potential plateau in the charge process is slightly changed. Especially, the potential polarization between the charge potential plateau and the low discharge potential plateau in the electrolyte with 5 M LiTFSI is larger (0.33V), normally at the discharge capacity of $400 \text{ mAh g}^{-1}(\text{composite})$. Correspondingly, the initial discharge capacities of the multi-composite are 870, 889, and 860 $\text{mAh g}^{-1}(\text{composite})$, respectively, in the electrolyte with increasing lithium salt concentration from 1M to 3 M and 5 M (LiTFSI). After 3 cycles, it seems that the charge and discharge capacities of the multi-composite in the electrolyte with 5 M LiTFSI are more stable.

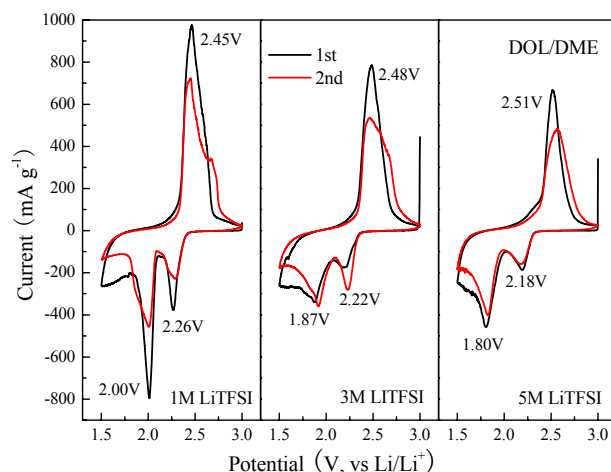


Fig. 6 Typical cyclic voltammograms of the as-prepared multi-composites with 51 wt % S in the electrolyte with 1M, 3M, 5M LiTFSI in DOL/DME at a scan rate of 0.1 mV s^{-1} .

Typical cyclic voltammograms (CVs) of the as-prepared multi-composites with 51 wt % S in the electrolyte with different concentrated lithium salts (LiTFSI) in DOL/DME are shown in Fig. 6. It is found from CVs that there are two cathodic peak potentials of 2.26 and 2.00 V (vs Li/Li⁺) for the composite in the electrolyte with 1 M LiTFSI due to the two-step reduction of sulfur in the presence of Li ions. With increasing the lithium salt

concentration in the electrolyte, the cathodic peak potentials are gradually shifted down to 2.22 and 1.87 V (vs Li/Li⁺) in the electrolyte with 3 M LiTFSI, and further down to 2.18 and 1.80 V (vs Li/Li⁺) in the electrolyte with 5 M LiTFSI. More sensitively, the anodic oxidation peak potentials are shifted up to 2.51 (vs Li/Li⁺) from 2.45 V (vs Li/Li⁺) with increasing the lithium salt concentration in the electrolyte, confirming a relatively high potential polarization, in analogy with the potential change in the charge/discharge curves. It means that the high concentration lithium salt (LiTFSI) in the electrolyte may alter the thermodynamic stabilization of the soluble lithium polysulfides as intermediates.

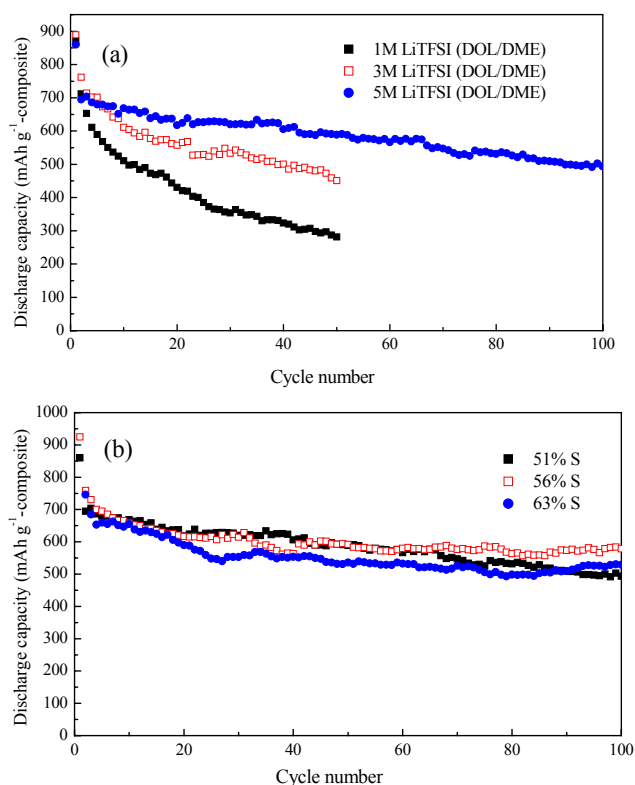


Fig. 7 (a) The cycle performance of the as-prepared multi-composite with 51 wt % S at the current density of 100 mA g⁻¹ in the electrolyte with 1M, 3M, 5M LiTFSI in DOL/DME. (b) The cycle performance of the as-prepared multi-composites with the different sulfur content in the electrolyte with 5 M LiTFSI in DOL/DME at the current density of 100 mA g⁻¹.

The long cycle stability of the multi-composite in the electrolyte with different concentrated lithium salt (LiTFSI) in DOL/DME can be shown in Fig. 7. Apparently, the high concentration lithium salt (LiTFSI) has a great impact on the cycle stability of the multi-composite by suppressing polysulfide dissolution due to common-ion effect.³⁸ As anticipated, after 100 cycles, the discharge capacity of 493.7 mAh g⁻¹(composite) is retained, when the multi-composite is cycled in the electrolyte with 5 M LiTFSI. While, the discharge capacity is quickly decreased to 281 mAh g⁻¹(composite) for the multi-composite after 50 cycles in the electrolyte with 1 M LiTFSI. When the multi-composites with 56 and 63 % S are cycled in the electrolyte with 5 M LiTFSI, the almost same cycle stability is still obtained with the discharge capacities of 578.1, and 528.7 mAh g⁻¹(composite)

after 100 cycles, respectively. Therefore, the high concentration lithium salt (LiTFSI) is in favor of the cycle stability at the slight expense of the discharge potential plateaus (width and height). It is noted that the multi-composite with 56 % S presents the best performance based on the evaluation of the discharge capacity, implying the high utilization of the active sulfur in the composite with 56 wt % S.

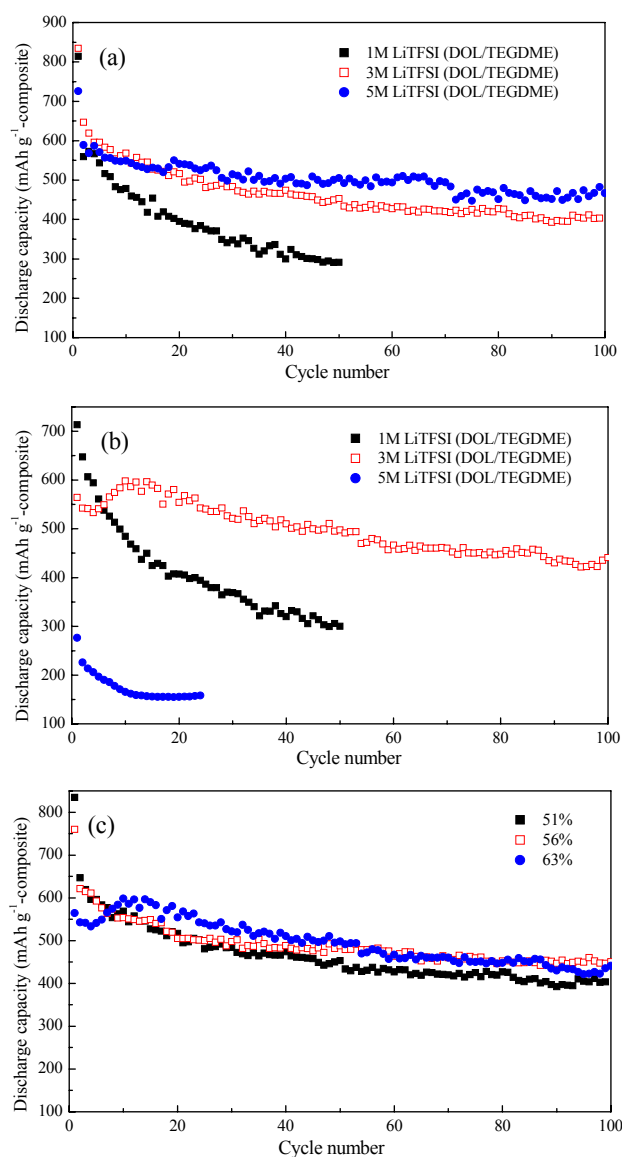


Fig. 8 The cycle performance of the multi-composites with 51 wt % S (a) and 63 wt % S (b) in the electrolyte with 1M, 3M, 5M LiTFSI in DOL/TEGDME at the current density of 100 mA g⁻¹. (c) The cycle performances of the multi-composites with the different sulfur content in electrolyte with 3 M LiTFSI in DOL/TEGDME at the current density of 100 mA g⁻¹.

It should be noted that the viscosity of the electrolyte also has a notable influence on the cycle stability of sulfur cathode.³⁹ When the lower viscous DME solvent is replaced by the higher viscous TEGDME solvent in the electrolyte,^{31,42,44} the cycle performance is obviously varied for the as-prepared multi-composites with different sulfur contents, as indicated in Fig. 8. For the multi-composite with 51 % S, the best cycle performance

is also obtained in the electrolyte with 5 M LiTFSI. On the contrary, the discharge capacity is much low for the multi-composite with 63 % S in the electrolyte with 5 M LiTFSI, while the cycle stability is poor in the electrolyte with 1 M LiTFSI. Concerning the evaluation of the discharge capacity and cycle stability, the multi-composite with 63 % S presents the optimized performance in the electrolyte with 3 M LiTFSI. The analogous performance is also observed in the multi-composite with 56 % S. Therefore, the electrochemical performance of the as-prepared multi-composites is dominated by both the lithium salt concentration and the solvent viscosity in the electrolyte.

Both the thermodynamics and kinetics of the electrode reaction are determined by the chemistry of the oxidized and reduced species in solution,⁴⁷ which is also the same with the sulfur electrode reaction based on the dissolution-deposition processes in organic electrolyte.⁴⁸ Any change to the solution composition that leads to thermodynamic stabilization of the oxidized or reduced species will make the reduction more difficult or easier, leading to a negative or positive shift in the formal potential.⁴⁷ The polysulfide dissolution process is thermodynamically favourable, and the electrolyte with high concentration lithium salt (LiTFSI) has thermodynamic and kinetic benefits to control the dissolution of polysulfide by the common ion effect,³⁹ causing the negative shift in the formal potential as demonstrated in Fig. 6. Generally, there is an opposite change in the viscosity and ionic conductivity of the electrolyte.⁴⁹ As shown in Table 1, the viscosity of the electrolyte is dramatically increased with increasing the lithium salt concentration, accompanying with the decrease of the ionic conductivity of the electrolyte. When the lower viscous DME solvent is replaced by the higher viscous TEGDME solvent in the electrolyte, the viscosity of the electrolyte could be hugely increased and the ionic conductivity of the electrolyte is also reduced. Correspondingly, the negative shift of the reduction potentials and the positive shift of the oxidation potential are more serious, when DME is replaced by TEGDME as indicated in Fig. 9. And the cathodic/anodic peak current is relatively lower, implying the corresponding low capacity of the composite in the electrolyte with the TEGDME component as shown in Fig. 8. Meanwhile, the polarization between the charge potential plateau and the low discharge potential plateau in the electrolyte with the higher viscous TEGDME solvent is relatively larger (Fig. S1). In particular, the discharge capability of the composite in the large current density is inevitably decreased. For example, at the current density of 1000 mA g⁻¹, the discharge capacity of the composite with 51 wt % S is obviously decreased, and discharge potential plateau is sloped with increasing the lithium salt concentration in the electrolyte, due to the increase of the viscosity and the decrease of the ionic conductivity in the electrolyte (Fig. S2). Therefore, the viscosity and the ionic conductivity in the electrolyte by adjusting the lithium salt concentration and solvent should be simultaneously compatible and optimized based on the requirement of the capacity, cycle stability and high rate capability of the sulfur cathode.

It should be noted here that the lithium ion binds more strongly to ether oxygens of TEGDME than DME,⁵⁰ as shown in Fig.10. When the lithium salt concentration is increased or the high viscous solvent is introduced, such interaction in the

complex is more strong, resulting in the consequent viscosity increase of the electrolyte. In the multi-step discharge process of the sulfur cathode, the dissolution of intermediate lithium polysulfides is unavoidable. Subsequently, the bulky long-chain polysulfide anions could join the interaction of the lithium salt and solvent, leading to further increase of the viscosity in the electrolyte. In the electrolyte with the moderate viscosity and ionic conductivity, such as 3 M LiTFSI DOL/TEGDME and 5 M LiTFSI DOL/DME, both the high discharge capacity and long cycle stability can be obtained for all the composites. On the contrary, the composite with a high sulfur content (63 wt %) could not deliver the high capacity in the electrolyte with the ultrahigh viscosity, such as 5 M LiTFSI DOL/TEGDME. By comparison, the increase of the viscosity in the electrolyte is more economically suitable for the high viscous solvent rather than the high concentration lithium salt.

Table 1 The shear viscosity and ionic conductivity of the different electrolytes.

electrolyte	Shear viscosity (η , mPa s, at 25°C)	ionic conductivity (σ , mS cm ⁻¹ at RT)
1M LiTFSI in DOL/DME	2.03	11.93
3M LiTFSI in DOL/DME	8.80	6.74
5M LiTFSI in DOL/DME	31.88	3.49
1M LiTFSI in DOL/TEGDME	4.58	8.64
3M LiTFSI in DOL/TEGDME	17.86	6.48
5M LiTFSI in DOL/TEGDME	68.65	1.94

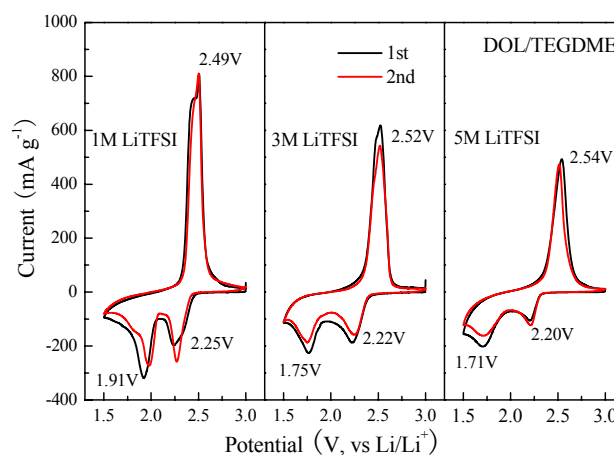


Fig. 9 Typical cyclic voltammograms of the as-prepared multi-composites with 51 wt % S in the electrolyte with 1M, 3M, 5M LiTFSI in DOL/TEGDME at a scan rate of 0.1 mV s⁻¹.

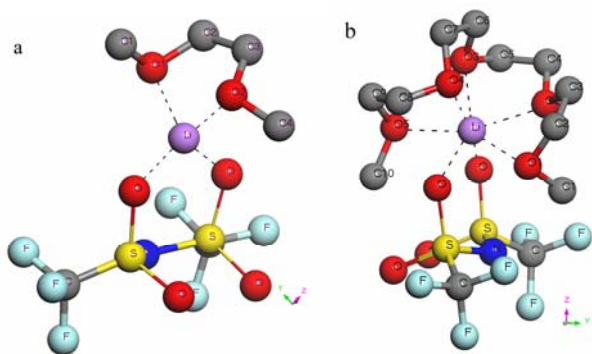


Fig. 10 The geometrical scheme of DME-Li⁺-TFSI⁻ (a) and TEGDME-Li⁺-TFSI⁻ (b).

5 Conclusions

In summary, sulfur/polyacrylonitrile(PAN)/carbon multi-composites are prepared by fixing sulfur on the matrix of the partially carbonized PAN (cPAN) and activated-conductive carbon black (A-CCB). Here, the dual-mode of fixing sulfur is presented in the multi-composites with chemically bonding to the PAN-derived backbone and physically loading on the matrix of both cPAN and A-CCB, which is beneficial for loading high sulfur as well as ensuring good conductivity of the multi-composite. It is demonstrated that the as-prepared multi-composites as active materials present the good electrochemical performance, especially in the optimized electrolyte with a high concentrated LiTFSI in different mixed solvents of DOL/DME or DOL/TEGDME. In particular, both the high concentration lithium salt and high viscous solvent have a great impact on the cycle stability of the multi-composite. Therefore, the electrochemical performance of the as-prepared multi-composites is obviously influenced by the common ion effect and viscosity of the electrolyte, which are induced from both the lithium salt and solvent. In future, an actual cell system with the high concentration lithium salt and high viscous solvent will be conducted to understand practical limitations and effects on the capacity and cycle stability of Li/S battery.

Acknowledgements

Financial Supports from the 863 Program (2011AA11A256), and NSFC (51072083) of China are gratefully acknowledged.

Notes and references

Institute of New Energy Material Chemistry, Collaborative Innovation Center of Chemical Science and Engineering (Tianjin), Tianjin Key Laboratory of Metal and Molecule Based Material Chemistry, Nankai University, Tianjin 300071, China. Fax: +86-22-23500876; Tel: +86-22-23500876; E-mail: xpgao@nankai.edu.cn

† Electronic Supplementary Information (ESI) available: The initial charge-discharge curves and high rate capability of the electrodes in the electrolyte with the different lithium salt concentration in DOL/TEGDME. See DOI: 10.1039/b000000x/

- X. L. Ji and L. F. Nazar, *J. Mater. Chem.*, 2010, 20, 9821.
- X. P. Gao and H. X. Yang, *Energy Environ. Sci.*, 2010, 3, 174.

- P. G. Bruce, S. A. Freunberger, L. J. Hardwick and J. M. Tarascon, *Nat. Mater.*, 2012, 11, 19.
- D. W. Wang, Q. C. Zeng, G. M. Zhou, L. C. Yin, F. Li, H. M. Cheng, I. R. Gentle and G. Q. Lu, *J. Mater. Chem. A*, 2013, 1, 9382.
- S. S. Zhang, *J. Power Sources*, 2013, 231, 153.
- R. D. Rauh, K. M. Abraham, G. F. Pearson, J. K. Surprenant and S. B. Brummer, *J. Electrochem. Soc.*, 1979, 126, 523.
- J. Shim, K. A. Striebel and E. J. Cairns, *J. Electrochem. Soc.*, 2002, 149, A1321.
- X. L. Ji, K. T. Lee and L. F. Nazar, *Nat. Mater.*, 2009, 8, 500.
- C. Lai, X. P. Gao, B. Zhang, T. Y. Yan and Z. Zhou, *J. Phys. Chem. C*, 2009, 113, 4712.
- B. Zhang, C. Lai, Z. Zhou and X. P. Gao, *Electrochim. Acta*, 2009, 54, 3708.
- B. Zhang, X. Qin, G. R. Li and X. P. Gao, *Energy Environ. Sci.*, 2010, 3, 1531.
- G. He, X. L. Ji and L. Nazar, *Energy Environ. Sci.*, 2011, 4, 2878.
- S. C. Wei, H. Zhang, Y. Q. Huang, W. K. Wang, Y. Z. Xia and Z. B. Yu, *Energy Environ. Sci.*, 2011, 4, 736.
- L. W. Ji, M. M. Rao, S. Aloni, L. Wang, E. J. Cairns and Y. G. Zhang, *Energy Environ. Sci.*, 2011, 4, 5053.
- G. M. Zhou, D. W. Wang, F. Li, P. X. Hou, L. C. Yin, C. Liu, G. Q. Lu, I. R. Gentle and H. M. Cheng, *Energy Environ. Sci.*, 2012, 5, 8901.
- W. H. Zhang, D. Qiao, J. X. Pan, Y. L. Cao, H. X. Yang and X. P. Ai, *Electrochim. Acta*, 2013, 87, 497.
- X. F. Wang, X. P. Fang, X. W. Guo, Z. X. Wang and L. Q. Chen, *Electrochim. Acta*, 2013, 97, 238.
- H. Ye, Y. X. Yin, S. Xin and Y. G. Guo, *J. Mater. Chem. A*, 2013, 1, 6602.
- H. S. Ryu, J. W. Park, J. Park, J. P. Ahn, K. W. Kim, J. H. Ahn, T. H. Nam, G. Wang and H. J. Ahn, *J. Mater. Chem. A*, 2013, 1, 1573.
- J. L. Wang, J. Yang, J. Y. Xie and N. X. Xu, *Adv. Mater.*, 2002, 14, 963.
- F. Wu, J. Z. Chen, R. J. Chen, S. X. Wu, L. Li, S. Chen and T. Zhao, *J. Phys. Chem. C* 2011, 115, 6057.
- L. F. Xiao, Y. L. Cao, J. Xiao, B. Schwenzer, M. H. Engelhard, L. V. Saraf, Z. M. Nie, G. J. Exarhos and J. Liu, *Adv. Mater.*, 2012, 24, 1176.
- Y. Z. Fu, Y. S. Su and A. Manthiram, *J. Electrochem. Soc.* 2012, 159, A1420.
- L. Wang, X. M. He, J. J. Li, J. Gao, J. W. Guo, C. Y. Jiang and C. R. Wan, *J. Mater. Chem.* 2012, 22, 22077.
- L. Wang, X. M. He, J. J. Li, M. Chen, J. Gao and C. Y. Jiang, *Electrochim. Acta* 2012, 72, 114.
- F. Wu, J. Z. Chen, L. Li, T. Zhao and R. J. Chen, *J. Phys. Chem. C* 2011, 115, 24411.
- G. C. Li, G. R. Li, S. H. Ye and X. P. Gao, *Adv. Energy Mater.*, 2012, 2, 1238.
- L. C. Yin, J. L. Wang, F. J. Lin, J. Yang and Y. N. Nuli, *Energy Environ. Sci.*, 2012, 5, 6966.
- X. Liang, Z. Y. Wen, Y. Liu, H. Zhang, J. Jin, M. F. Wu and X. W. Wu, *J. Power Sources* 2012, 206, 409.
- M. M. Rao, X. Y. Song, H. G. Liao and E. J. Cairns, *Electrochim. Acta*, 2012, 65, 228.
- W. Wang, G. C. Li, Q. Wang, G. R. Li, S. H. Ye and X. P. Gao, *J. Electrochem. Soc.*, 2013, 160, A805.
- L. X. Miao, W. K. Wang, A. B. Wang, K. G. Yuan and Y. S. Yang, *J. Mater. Chem. A*, 2013, 1, 11659.
- T. N. L. Doan, M. Ghaznavi, Y. Zhao, Y. G. Zhang, A. Konarov, M. Sadhu, R. Tangirala and P. Chen, *J. Power Sources*, 2013, 241, 61.
- J. Fanous, M. Wegner, M. B. M. Spera and M. R. Buchmeiser, *J. Electrochem. Soc.*, 2013, 160, A1170.
- J. Fanous, M. Wegner, J. Grimming, M. Rolff, M. B. M. Spera, M. Tenzer and M. R. Buchmeiser, *J. Mater. Chem.*, 2012, 22, 23240.
- L. C. Yin, J. L. Wang, X. L. Yu, C. W. Monroe, Y. NuLi and J. Yang, *Chem. Commun.*, 2012, 48, 7868.
- Y. G. Zhang, Y. Zhao, A. Yermukhambetova, Z. Bakenov and P. Chen, *J. Mater. Chem. A*, 2013, 1, 295.
- E. S. Shin, K. Kim, S. H. Ohand and W. I. Cho, *Chem. Commun.*, 2013, 49, 2004.

- 39 L. M. Suo, Y. S. Hu, H. Li, M. Armand and L.Q. Chen, *Nat. Commun.*, 2013, 4, 1481.
- 40 J. T. Lee, Y. Zhao, S. Thieme, H. Kim, M. Oschatz, L. Borchardt, A. Magasinski, W. I. Cho, S. Kaskel and G. Yushin, *Adv. Mater.*, 2013, 25, 4573.
- 5 41 J. T. Lee, Y. Y. Zhao, H. Kim, W. I. Cho and G. Yushin, *J. Power Sources*, 2014, 248, 752.
- 42 J. W. Choi, J. K. Kim, G. Cheruvally, J. H. Ahn, H. J. Ahn and K. W. Kim, *Electrochim. Acta*, 2007, 52, 2075.
- 10 43 C. Barchasz, J. C. Lepretre, S. Patoux and F. Alloin, *J. Electrochem. Soc.*, 2013, 160, A430.
- 44 C. Barchasz, J. C. Lepretre, S. Patoux and F. Alloin, *Electrochim. Acta*, 2013, 89, 737.
- 45 G. C. Li, J. J. Hu, G. R. Li, S. H. Ye and X. P. Gao, *J. Power Sources*, 2013, 240, 598.
- 15 46 X. G. Yu, J. Y. Xie, Y. Li, H. J. Huang, C. Y. Lai and K. Wang, *J. Power Sources*, 2005, 146, 335.
- 47 D. Pletcher, *A First Course in Electrode Processes*, 2nd edition, The Royal Society of Chemistry, 2009.
- 20 48 J. J. Hu, G. R. Li and X. P. Gao, *J. Inorg. Mater.*, 2013, 28, 1181.
- 49 J. M. Zheng, M. Gu, H. H. Chen, P. Meduri, M. H. Engelhard, J. G. Zhang, J. Liu and J. Xiao, *J. Mater. Chem. A*, 2013, 1, 8464.
- 50 T. V. Kaulgud, N. R. Dhumal and S. P. Gejji, *J. Phys. Chem. A* 2006, 110, 9231.
- 25